
Lateralized Differences in Iodine-123-IBZM Uptake in the Basal Ganglia in Asymmetric Parkinson's Disease

Michael B. Knable, Douglas W. Jones, Richard Coppola, Thomas M. Hyde, Kan Sam Lee, Julia Gorey and Daniel R. Weinberger

Clinical Brain Disorders Branch, National Institutes of Health, Bethesda, Maryland; and Intramural Research Program, National Institute of Mental Health, Neuroscience Center at St. Elizabeths Hospital, Washington, D.C.

We used equilibrium analysis of SPECT data from patients with asymmetric Parkinson's disease to determine if lateralized differences in the striatal uptake of [¹²³I]IBZM correlate with asymmetry in clinical findings and, by inference, with lateralized differences in the concentration of extracellular dopamine. **Methods:** Twelve patients with asymmetric clinical signs of idiopathic Parkinson's disease were injected with a bolus of [¹²³I]IBZM, and multiple SPECT scans recorded the time course of radioligand uptake. The time integral method was used to estimate peak specific binding, so that a ratio of specific-to-nonspecific binding in the left and right striatum of each subject at equilibrium could be determined. Nine patients also had ^{99m}Tc-HMPAO SPECT scans which were examined for evidence of blood flow asymmetries. **Results:** Paired t-tests comparing [¹²³I]IBZM uptake revealed significantly greater (mean = 7.3%) availability of dopamine-D2 receptors in the basal ganglia contralateral to maximal clinical signs. Differences in receptor availability correlated significantly with differences in every measure of the clinical assessment. No significant differences in regional cerebral blood flow between the two sides were observed with ^{99m}Tc-HMPAO. **Conclusion:** These results demonstrate the ability of [¹²³I]IBZM SPECT to reveal clinically meaningful variations in striatal dopamine receptor availability in patients with asymmetric Parkinson's disease. The equilibrium analysis technique used to determine these findings is a simple and robust method of measuring relative receptor availability and may be useful in studying other illnesses where dysfunction of dopaminergic neurotransmission is suspected.

Key Words: Parkinson's disease; iodine-123-IBZM; single-photon emission computed tomography; dopamine receptors

J Nucl Med 1995; 36:1216-1225

In vitro, ex vivo and in vivo studies in animals with (S)-(-)-2-hydroxy-3-iodo-6-methoxy-N[(1-ethyl-2-pyrrolidinyl)methyl] benzamide (IBZM) have demonstrated the

high affinity and specificity of this compound as a dopamine-D2 receptor antagonist (1-4). SPECT with [¹²³I]IBZM in humans demonstrates relatively selective striatal uptake (5-7). Furthermore, the long radioactive half-life (13.2 hr) and favorable kinetic behavior of [¹²³I]IBZM allows for time course studies extending over a period of hours. Such studies have demonstrated, for example, displacement of [¹²³I]IBZM when amphetamine is administered intravenously during SPECT studies (8,9), a finding thought to reflect increased levels of endogenous dopamine stimulated by amphetamine. This observation indicates that [¹²³I]IBZM uptake might be a useful measure of in vivo dopamine receptor availability, an availability determined not merely by receptor density but also by the dynamic interplay of these receptors with naturally occurring endogenous dopamine.

Patients with clinically asymmetric parkinsonism are excellent subjects on which to test SPECT's ability to probe in vivo dopamine receptor availability and, in particular, the role of endogenous dopamine in determining this availability. Although the relative contributions of endogenous dopamine and dopamine receptor density to the outcome measurements of a single, high-specific activity SPECT scan session cannot be absolutely discriminated, this study was designed in such a way as to maximize the potential role of endogenous transmitter. In asymmetric Parkinson's disease, the extracellular concentration of dopamine is presumed to be less in the striatum contralateral to maximal clinical signs when compared to the ipsilateral striatum. Postmortem human studies and studies of animals with nigrostriatal lesions have shown that the loss of nigrostriatal neurons is associated with an early increase in striatal D2 receptor density and that this "denervation supersensitivity" is reversed by treatment with dopaminergic drugs (10-13). For the subjects in this study who had dopaminergic drugs withheld for 48 hr, dopamine receptor availability was predicted to be greater in the contralateral striatum primarily on the basis of decreased concentrations of endogenous dopamine, since this period of drug abstinence is presumably insufficient to allow for dopamine receptors to upregulate.

Received Sept. 16, 1994; revision accepted Dec. 19, 1994.
For correspondence or reprints contact: Michael B. Knable, DO, Clinical Brain Disorders Branch, NIMH, Neuroscience Center at St. Elizabeths Hospital, 2700 Martin Luther King Jr. Ave., S.E., Washington, DC 20032.

The possibility of observing this asymmetry in dopamine receptor availability with [^{123}I]IBZM was sought with a subject comparison of right and left striata. This approach controls a number of confounding sources of variability including, individual differences in the somatic clearance rate of [^{123}I]IBZM, individual differences in mental state and variations in scanning circumstances. In spite of the controls inherent in this design, however, it is also necessary to have a valid and reproducible method of analyzing the [^{123}I]IBZM data which yields a meaningful measure of relative dopamine receptor availability. Towards this end, a simple linear regression analysis of the time integral of specifically bound [^{123}I]IBZM was introduced and employed. To determine whether the asymmetries observed by this method might merely reflect differences in tracer delivery due to asymmetric cerebral blood flow, $^{99\text{m}}\text{Tc}$ -HMPAO SPECT studies were analyzed for any indication of similar lateralization.

In general, previous [^{123}I]IBZM SPECT studies of parkinsonian patients have based their conclusions about dopamine function on data obtained at a single time point. Patients with idiopathic Parkinson's disease have striatal [^{123}I]IBZM activity in single scan paradigms that is similar to that in control subjects (14–17). A favorable response to apomorphine in patients with Parkinson's disease can also be predicted by normal striatal [^{123}I]IBZM activity (15–18). Normal striatal [^{123}I]IBZM activity is thought to reflect the presence of viable postsynaptic striatal neurons in patients with Parkinson's disease. In contrast, patients with poor and fluctuating responses to L-dopa (19), patients with Wilson's disease (20,21), patients with multiple system atrophy or progressive supranuclear palsy (22), and patients with Huntington's disease (23) have been shown to have lower than normal striatal [^{123}I]IBZM activity, perhaps reflecting pathological involvement of postsynaptic neurons in these disorders. These results must be viewed with some caution, however, since between-group comparisons of [^{123}I]IBZM activity is complicated by the above-mentioned sources of individual variation, especially when data are gathered at a single point in time.

One previous SPECT study demonstrated a significant increase in both the relative uptake and accumulation rate of [^{123}I]IBZM in the striatum contralateral to clinical symptoms in patients with asymmetric Parkinson's disease (24). The results of this study, however, were based on two SPECT acquisitions (at 15 and 90 min postinjection) rather than a more detailed time course data, and no attempt was made to correlate the asymmetry of [^{123}I]IBZM uptake with the degree of clinical asymmetry. Nevertheless, the majority of patients exhibited increased [^{123}I]IBZM activity in the contralateral striatum, which was interpreted as evidence of dopamine-D2 receptor upregulation in a series of dopamimetic-naïve patients. PET studies have also sought evidence of laterality in patients with asymmetric Parkinson's disease. One study with ^{11}C -raclopride in unmedicated patients found increased binding in the contralateral striatum (25), whereas a study of medicated and

unmedicated patients with ^{11}C -methylspiperone did not (26). We performed dynamic [^{123}I]IBZM SPECT studies in a series of medicated patients with asymmetric Parkinson's disease and hypothesized that an equilibrium analysis would demonstrate a lateralized difference in the number of unoccupied dopamine-D2 receptors (which is in part determined by the local concentration of endogenous dopamine), where single time point analyses have failed to do so.

MATERIALS AND METHODS

Patients

Patients were recruited from the local community and by an advertisement in the "Young People with Parkinson's Disease Association" newsletter. All of the patients had at least two of the four symptoms of idiopathic Parkinson's disease: tremor, bradykinesia, rigidity or postural instability. Patients were excluded if neurologic history and examination, brain MRI scans or laboratory tests suggested a clinical diagnosis other than idiopathic Parkinson's disease. Written informed consent for all procedures was obtained from each patient. All patients were examined independently by two neurologists following 48 hr of abstinence from dopamimetic drugs. Movement disorder severity was quantitated with the Hoehn and Yahr Scale (27) and by the Modified Abnormal Involuntary Movements Scale (AIMS) (28). The Modified AIMS scale includes clearly defined scales from 0 to 4 for chorea, dystonia, tremor, bradykinesia and rigidity. Based on the AIMS criteria, none of the patients had choreiform movements and five had dystonic posturing. Right and left side AIMS scores were summed separately and these total scores were used to define an asymmetry index (AI) as the absolute difference between the totals divided by their sum. Thus, AI values can range from 0.0 to 1.0 with unity corresponding to completely unilateral clinical signs. In order to be included in this study, patients were required to have an AI in excess of 0.33, i.e., the more severely affected side had to exhibit twice the total AIMS score of the less affected side. Patient demographic information and clinical ratings are presented in Table 1.

All patients had been exposed to antiparkinsonian medications and all had experienced symptomatic relief from these medications. For the purposes of this study, all patients consented to remain free of antiparkinsonian medications beginning 48 hr prior to the SPECT scanning sessions. This period of abstinence was felt to be long enough to remove confounding interactions between dopamimetic drugs and [^{123}I]IBZM uptake. On the other hand, this abstinence period is probably insufficient to allow for reupregulation of dopamine-D2 receptors, an effect suggested to occur in the absence of antiparkinsonian medications (10–13,29,30). Six patients had concurrent medical illness requiring additional medications which they continued to take during the course of this study. Table 2 summarizes the drug exposure history of the patients. To exclude patients with significant dementia or depression, the Folstein Mini-Mental Status Examination and the Hamilton Depression Rating Scale were administered. The 12 patients ultimately included in this study had mean scores on these examinations of 29.7 (range 28–30) and 6.0 (range 0–20), respectively.

Radlpharmaceuticals

Iodine-123-IBZM was prepared by the peracetic acid technique developed by Kung (31). Briefly, this is an oxidative iodination of

TABLE 1
Subject Demographics

Subject no.	Age (yr)	Sex	Illness duration (yr)	Hoehn and Yahr stage	Asymmetry index
1	38	M	6.0	II	0.41
2	58	F	0.5	I	1.00
3	74	M	3.5	I	1.00
4	67	M	6.0	II	0.41
5	43	F	6.0	II	0.74
6	43	M	3.0	I	1.00
7	61	M	1.5	I	1.00
8	56	M	9.0	I	1.00
9	44	F	2.0	II	0.80
10	59	M	6.0	II	0.39
11	45	M	7.0	II	0.97
12	59	M	1.0	I	1.00
mean ± s.d.	53.9 ± 11.1		4.3 ± 2.7		0.81 ± 0.26

BZM (S-(-)-N-[(1-ethyl-2-pyrrolidinyl)methyl]-2-hydroxy-6-methoxybenzamide) with carrier-free ^{123}I purchased in the form of sodium iodide (Nordion Intl., Vancouver, BC). Radiolabeled [^{123}I]IBZM was isolated by high-performance liquid chromatography (HPLC) on a reverse-phase column (PRP-1, Hamilton, Reno, NV) eluting at (1.0 ml/min) with acetonitrile-to-ammonium phosphate (4 mM, pH 7.0) 82% solvent (82:18). Prior to injection, the prepared radiopharmaceutical was sterilized by filtration through a 0.22- μm filter (Millipore, Bedford, MA). Periodic quality control tests have confirmed these preparations to be sterile and pyrogen-free. The overall radiochemical yield of this labeling procedure was greater than 50%, and radiopharmaceutical purity exceeded 95%. The specific activity of [^{123}I]IBZM prepared by this procedure is exceedingly high and may approach the carrier-free theoretical limit of 8.9×10^6 Gbq/mole (2.4×10^5 Ci/mole).

Technetium-99m-HMPAO was purchased from Amersham Intl. (Arlington Heights, IL) and was prepared and tested according to the manufacturer's specifications.

Data Acquisition

Volume acquisition SPECT scans were acquired by a CERASPECT dedicated brain camera (Digital Scintigraphics, Waltham, MA) with the gantry tilted 20° from vertical to allow subjects to recline comfortably during the extended time course studies. With the aid of a laser positioning beam, patients were positioned within the gantry with their canthomeatal lines parallel to the transverse axis of the SPECT camera. Iodine-123-IBZM scans were acquired in step-and-shoot mode for 120 projections. In addition to a photopeak window (145–175 keV), windows above (175–191 keV) and below (127–143 keV) it were also recorded and were subtracted from the photopeak window for scatter correction. The data were reconstructed with a Butterworth filter (cutoff = 1 cm, power factor = 10) and were displayed as a 64-slice \times 128 \times 128 volume comprised of isotropic voxels. The corresponding field of view was approximately 107 mm \times 213 mm \times 213 mm. The relatively low count rates and short scan durations of the time course studies required a high-sensitivity

TABLE 2
Subject Drug Exposure History

Subject no.	Anti-parkinsonian medications*	Exposure duration (yr)	Other medications at time of SPECT imaging
1	Se, Ld	2.0	None
2	Se, Tr	0.5	None
3	Ld	3.0	Sucralfate, digoxin, diltiazem
4	Se, Ld, Tr	6.0	Propranolol, nifedipine
5	Aa, Se	4.0	None
6	Se, Ld, Aa	3.0	None
7	Se, Ld, Ba	1.5	None
8	Se, Ld, Br	8.0	Alprazolam
9	Se, Pe, Ai	1.5	None
10	Se, Ld	5.0	Aspirin, metoprolol
11	Ld	5.0	Lisinopril
12	Se	0.5	Cholestyramine
mean ± s.d.		3.3 ± 2.3	

*Key to medications: Aa = Amantadine; Ai = Amitriptyline; Ba = Baclofen; Br = Bromocriptine; Ld = L-dopa/carbidopa; Pe = Pergolide; Se = Selegiline; and Tr = Trihexyphenidyl.

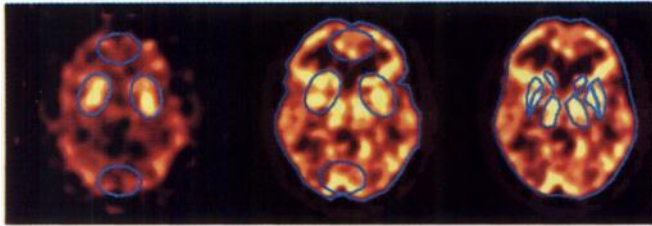


FIGURE 1. A representative example of an [¹²³I]IBZM SPECT scan (left) shows placement of ROIs. Also shown is the same subject's HMPAO-SPECT scan to which the ROIs used for [¹²³I]IBZM SPECT (center) and the MRI registered ROIs (right) have been applied.

collimator with roughly 11.5 mm FWHM resolution. No attenuation correction was performed on the [¹²³I]IBZM SPECT data, with the assumption that a comparison between the two sides of the brain would not be affected by attenuation.

For the [¹²³I]IBZM time course studies, injected activities averaged 192 MBq (5.2 mCi) and ranged from 170 MBq (4.6 mCi) to 237 MBq (6.4 mCi). To minimize the radiation exposure to the thyroid gland, each patient took 5 drops/day of oral Lugol's solution 1 day prior to [¹²³I]IBZM administration and for the next 3 days. The first SPECT scan began 15 min after intravenous bolus injection of [¹²³I]IBZM, and subsequently, a series of 15-min scans were acquired over a 4-hr period. Subjects were allowed to take breaks between scans if needed and no attempt was made to restrain the subjects' heads.

Nine of the twelve patients in this study volunteered for a ^{99m}Tc-HMPAO SPECT blood flow study. These studies were performed on the day preceding each patient's [¹²³I]IBZM to allow time for the ^{99m}Tc to decay but still be in close proximity to the time of the [¹²³I]IBZM study. Injected activities of ^{99m}Tc-HMPAO averaged 551 MBq (14.9 mCi) with a range of 536–555 MBq (14.5–15.0 mCi). A single 30-min SPECT scan was performed on each of these patients beginning 15 min after ^{99m}Tc-HMPAO was administered intravenously. Technetium-99m-HMPAO scans were acquired in the step-and-shoot mode for 120 projections. A scatter window (112–126 keV) was recorded and subtracted from the photopeak window (126–154 keV). The data were reconstructed with a Butterworth filter (cutoff = 0.75 cm, power factor = 10) and were displayed on 64 × 128 × 128 matrix. The static ^{99m}Tc-HMPAO scans were performed with a high-resolution collimator with roughly 7.5mm FWHM resolution. No attenuation correction was applied to the ^{99m}Tc-HMPAO scans.

Image Analysis

Each time point during the IBZM-SPECT procedure produced 64 images with a slice thickness of 1.67 mm. Five slices summed together contained the image with the highest signal in the region of the basal ganglia as the central slice. Elliptical regions of interest (ROIs) of identical cross-sectional areas (10 cm²) were drawn around each basal ganglia and at the posterior extent of the occipital cortex as illustrated in Figure 1. The calculated three-dimensional volume of the ROIs was 8.35 ml. To restrict measurements to gray matter voxels within the confines of each ellipse and to reduce artifacts related to partial voluming and patient movement between scans, only 10% of the pixels with highest counts in each ellipse (corresponding to a volume of 0.835 ml) was measured to determine the concentration of ¹²³I activity within each ROI. This method assumes the basal ganglia to have homogeneous [¹²³I]IBZM uptake and no anatomical redistribution during

the time period of the study. The ROI activity concentration data were corrected for radioactivity decay from the time of injection and normalized to the activity of the corresponding injected dose.

The ^{99m}Tc-HMPAO SPECT scans were analyzed by two methods to determine the extent to which blood flow effects might explain any observed differences in the [¹²³I]IBZM data. Prior to analysis, a volume MRI scan was coregistered with the ^{99m}Tc-HMPAO SPECT scan for each subject. MRI scans were obtained on a 1.5T Signa scanner (General Electric Medical Systems, Milwaukee, WI), with a spoiled GRASS sequence (TR = 24 msec, TE = 5 msec) that generated a set of 124 contiguous sagittal slices with a 1.5-mm slice thickness and an in-plane field of view of 240 mm across a 256 × 256 matrix. MRI volumes were scaled and aligned to match ^{99m}Tc-HMPAO SPECT scans using the "NIH Image" computer program (public domain). Rotations and translations were determined by comparing outlines and landmarks in three mutually orthogonal planes passing through the center of the brain. As had been done in analyzing the [¹²³I]IBZM SPECT scans, sums of five slices containing the greatest extent of the basal ganglia were calculated for both the MRI scans and the ^{99m}Tc-HMPAO SPECT scans. In the first method of analysis, ROIs were drawn on the summed MRI images to delineate left and right caudate, globus pallidus, putamen and thalamus. These anatomical ROIs were transferred to their corresponding summed ^{99m}Tc-HMPAO images and activity concentrations were measured. These measurements were normalized in two different ways: (1) to the injected dose activity and (2) to the average activity concentration of the entire portion of the image occupied by brain tissue.

For the second method of ^{99m}Tc-HMPAO image analysis, the same elliptical ROIs that had been applied to the summed [¹²³I]IBZM images were positioned on the summed ^{99m}Tc-HMPAO images, and the activity concentration of 10% of the voxels with the highest counts measured within each ellipse. The basal ganglia measurements obtained by this method were also normalized in two different ways: (1) to the injected dose activity and (2) to the activity concentration obtained from the occipital ROI. All the ^{99m}Tc-HMPAO measurements were classified as either contralateral or ipsilateral to maximal clinical signs and were compared using matched-pair, two-tailed, Student's t-tests. Possible correlations with the [¹²³I]IBZM data were also tested for this latter set of ^{99m}Tc-HMPAO data whose measurement most closely mimicked the ROI analysis of the [¹²³I]IBZM images by applying Spearman's rank correlation and Pearson's linear correlation tests.

Data Analysis: Theoretical Aspects

SPECT data were analyzed with an equilibrium technique modified from previous work (32,33); however, the modifications used in this study require further explanation. The concentration of specifically bound radioligand is described by the familiar rate equation (34),

$$\frac{dC_b(t)}{dt} = k_{on} \cdot C_f(t) \cdot B_{unocc} - k_{off} \cdot C_b(t), \quad \text{Eq. 1}$$

where $C_b(t)$ is the concentration of specifically bound radioligand; $C_f(t)$ is the concentration of free radioligand; k_{on} and k_{off} are the association and dissociation rate constants, respectively; and B_{unocc} is the concentration of receptors which are unoccupied by endogenous neurotransmitter and, therefore, available for radioligand binding.

Since [¹²³I]IBZM does not bind irreversibly, the concentration

of bound radioligand, $C_b(t)$, will achieve a peak value at some time, t_p . At this maximum of specific binding, a transient equilibrium between association and dissociation exists and the derivative in Equation 1 vanishes leaving:

$$C_b(t_p) = C_f(t_p) \cdot B_{unocc}/K_d, \quad \text{Eq. 2}$$

where $K_d = k_{off}/k_{on}$ is the equilibrium dissociation constant. The concentration of free radioligand, $C_f(t)$ is assumed to be some constant fraction, f , of the total concentration of free and nonspecifically bound ligand, i.e., the nondisplaceable radioligand, $C_{nd}(t)$. The concentration of radioligand measured in occipital cortex, $C_{occ}(t)$, was used to approximate $C_{nd}(t)$ in the striatum. Finally, since SPECT measurements of striatal activity reflect the total radioligand concentration, $C_{str}(t) = C_b(t) + C_{nd}(t)$, Equation 2 becomes:

$$\frac{C_{str}(t_p) - C_{occ}(t_p)}{C_{occ}(t_p)} = f \cdot B_{unocc}/K_d. \quad \text{Eq. 3}$$

In this study, an analysis technique was developed which provides a means of applying Equation 3 reliably. First, the concentration measured in the occipital cortex is subtracted from that measured in the striata to obtain the specific binding in the striata as a function of time, $C_b(t) = C_{str}(t) - C_{occ}(t)$. Next, this estimate of specific binding was numerically integrated by the trapezoid rule to yield a curve of the integral of the specific binding as a function of time:

$$I_b(t_n) = \int_{t_0}^{t_n} dt \cdot C_b(t) \approx \sum_{i=1}^n (t_i - t_{i-1}) \cdot \frac{1}{2} \cdot [C_b(t_i) + C_b(t_{i-1})]. \quad \text{Eq. 4}$$

The integral of the specific binding, $I_b(t)$, is a sigmoidal function of time that achieves its maximal slope at the time, t_p , when peak specific binding occurs. The integral curve is nearly linear at this time and its slope is, in fact, equal to the peak value of the specific binding curve:

$$I_b(t) \approx C_b(t_p) \cdot t + (\text{constant}), \text{ for } t \approx t_p. \quad \text{Eq. 5}$$

In this study, data points which fell within the linear portion of the integral curve were chosen by visual inspection. Points at either end of the time integral curve were excluded when they deviated from a straight line. A least-squares linear regression analysis for the slope of the line through the selected data points provides an estimate of the peak specific binding, $C_b(t_p)$. In applying this method to within-subject comparisons of the left and right striata, the same time points were chosen for both striata of each subject. Both the number of points and their location in time were judged separately from subject to subject to allow for individual variations in the shape and peak position of the specific binding curve.

Once $C_b(t_p)$ was determined, an estimate of the occipital cortex activity at the time of peak specific binding, $C_{occ}(t_p)$, was made to obtain $f \cdot B_{unocc}/K_d$. The average of several occipital cortex points straddling the midpoint of the linear portion of the integral curve was used as this estimate. If the linear portion of the integral curve contained an odd number of points, then three points, (the midpoint and one to each side), were included in the average; for an even number of points, the two points straddling the midpoint were averaged.

The major goal of the integral curve method is to optimally

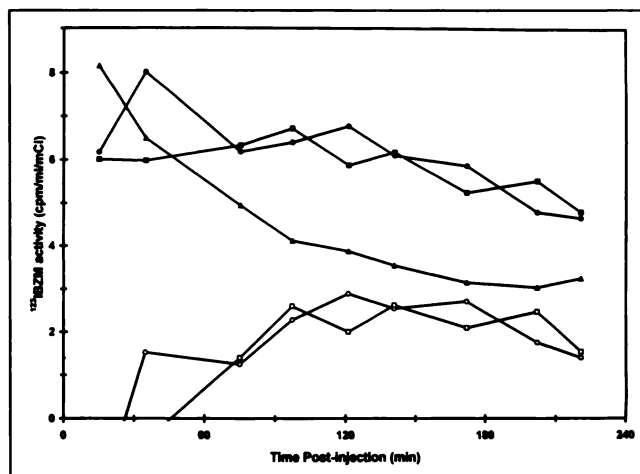


FIGURE 2. A typical set of [^{123}I]BZM time-activity curves illustrating total uptake in the right striatum (\bullet), the left striatum (\blacksquare) and the occipital cortex (\blacktriangle), and the specific binding curves estimated by subtracting the occipital measurements from the total curves for the right striatum (\circ) and the left striatum (\square).

select data points to be included in the equilibrium outcome measure. Examination of Figures 2 and 3 will highlight the advantages of this method of estimating the peak specific binding. As seen in Figure 2, the selection of any one data point as the peak may reveal a chance lateralized difference in striatal IBZM uptake because of the random fluctuations in the specific binding curve. Estimation of peak specific binding made by choosing a priori an elapsed time from injection may also generate spurious results because of the between-subject variability in time to peak specific binding of dopamine receptor radioligands (7,33).

Since the selection of "linear" points is based on visual inspection, an inter-rater reliability study of this method was performed. Two raters blinded to the side with maximal clinical signs inde-

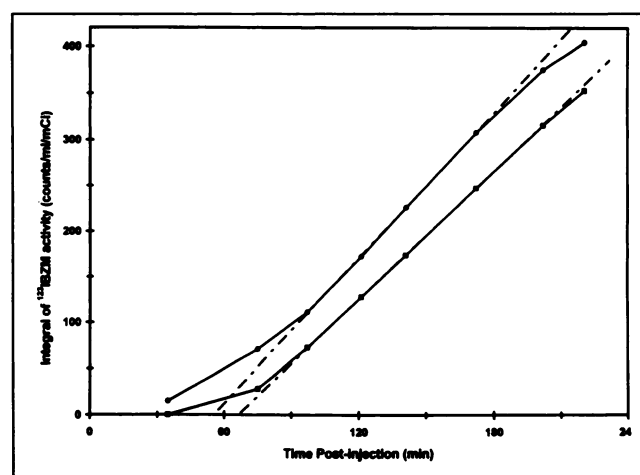


FIGURE 3. The time integrals of the [^{123}I]BZM specific binding curves shown in Figure 2 for the right striatum (\bullet), and the left striatum (\blacksquare). For this patient, maximal clinical signs were observed on the left side of the body. The linear regression lines used to calculate the peak specific binding from the slope are indicated by broken lines, and the slightly steeper slope for the striatum contralateral to maximal symptoms is apparent. Slopes were calculated for both sides of the brain using the third through the sixth data points.

TABLE 3
 Basal Ganglia Values of $f\text{-}B_{\text{unocc}}/K_d$ for Iodine-123-IBZM Obtained by the Slope of Integral and the Single-Scan at Two Hours Methods

Subject no.	Integral method		Single-scan method	
	Contralateral	Ipsilateral	Contralateral	Ipsilateral
1	0.465	0.508	0.494	0.453
2	1.165	1.170	0.937	1.087
3	0.274	0.218	0.278	0.320
4	0.309	0.399	0.439	0.406
5	1.679	1.451	0.785	0.571
6	1.573	1.376	1.412	1.519
7	0.713	0.627	0.736	0.522
8	0.537	0.493	0.644	0.620
9	0.570	0.478	0.565	0.501
10	0.735	0.606	0.615	0.708
11	0.811	0.778	0.952	0.984
12	0.466	0.429	0.531	0.435
mean \pm s.e.m.	0.775 \pm 0.134	0.711 \pm 0.116	0.699 \pm 0.086	0.677 \pm 0.101
p value	0.034		0.527	

pendently selected the linear points for each of the 24 integral curves. The agreement between the two sets of linear regression slopes was highly significant: the unbiased intraclass correlation coefficient (35) was 0.990 and the Pearson's linear correlation coefficient was 0.992 with vanishingly small p-values for both coefficients.

The values $f\text{-}B_{\text{unocc}}/K_d$ for each striatum were classified as being either contralateral or ipsilateral to the side of maximum clinical signs and compared with a matched pair, two-tailed Student's t-test. Right-left difference scores were also analyzed for correlations with lateralized differences in clinical signs by means of Spearman's rank correlation coefficient and Pearson's linear correlation coefficient. Additionally, to test the hypothesis that these results might have been obtained by analysis of data from a single SPECT scan at 2 hr, data corresponding to a 2-hr time point was estimated by linear interpolation between the two time points nearest to 2 hr in the actual time-activity curves. Direct substitution of these data into Equation 3 yielded values of $f\text{-}B_{\text{unocc}}/K_d$ based on the assumption that peak specific binding was evident in all subjects at 2 hr; these data were subjected to the same comparisons discussed above.

RESULTS

A representative plot of [^{123}I]IBZM time-activity data from one study is shown in Figure 2. [^{123}I]IBZM characteristically exhibited a broad peak of specific binding between 90 min and 210 min and a smooth washout of non-specific activity. Figure 3 is a plot of the integral of [^{123}I]IBZM activity as a function of time as calculated from the specific binding curves of Figure 2. The linear portions of these slightly sigmoidal curves are evident, as is the greater slope of the regression line corresponding to the right striatum which is contralateral to maximal clinical signs in this patient. The midpoints of the linear portions of these curves for the 12 patients revealed that peak specific binding of [^{123}I]IBZM in the basal ganglia occurred at times ranging from 93 min to 158 min postinjection (mean \pm s.d. = 127 \pm 22 min).

Values of $f\text{-}B_{\text{unocc}}/K_d$ were calculated according to

Equation 3 for both basal ganglia of each subject, classified as contralateral or ipsilateral to maximal clinical signs, and compared via matched pair, two-tailed Student's t-tests. The values obtained using the integral method revealed a significantly ($t = 2.42$, $p = 0.034$) greater mean value of $f\text{-}B_{\text{unocc}}/K_d$ for the contralateral basal ganglia (mean \pm s.e.m. = 0.775 \pm 0.134), than for the ipsilateral basal ganglia (mean \pm s.e.m. = 0.711 \pm 0.116). Only three of twelve patients failed to follow this pattern as shown in Table 3. Values obtained using the simulated single scan at two hours are also reported in Table 3. This method failed to find significance ($t = 0.65$, $p = 0.52$) in the difference between $f\text{-}B_{\text{unocc}}/K_d$ values for the contralateral basal ganglia (mean \pm s.e.m. = 0.699 \pm 0.086), and for the ipsilateral basal ganglia (mean \pm s.e.m. = 0.677 \pm 0.101). Furthermore, five of the twelve patients had ipsilateral values which exceeded the contralateral values. Patients with higher contralateral values did not significantly differ from patients with higher ipsilateral values in terms of age, asymmetry index, illness duration or duration of drug exposure in either method of analysis. Values obtained by the integral method, however, were significantly correlated with those obtained by the simulated single scan (Spearman's $\rho = 0.916$, $p < 0.001$ for the contralateral striatum and $\rho = 0.825$, $p < 0.001$ for the ipsilateral striatum).

The difference between the right and left basal ganglia $f\text{-}B_{\text{unocc}}/K_d$ values determined by the integral method also correlated significantly with clinical measures of disease lateralization. For correlational analyses, right-sided scores for total AIMS and for tremor, rigidity, bradykinesia and dystonia subscales, were subtracted from scores for the left side of the body. Table 4 summarizes the results of this analysis. The Spearman's rank correlation test revealed that differences in $f\text{-}B_{\text{unocc}}/K_d$ correlated significantly with the differences in total AIMS score and the four subscales (total AIMS: $\rho = 0.82$, $p = 0.0012$; tremor:

TABLE 4
Correlations between Lateralized Differences in Clinical Ratings and Basal Ganglia Values of $f\text{-}B_{\text{unocc}}/K_d$ for Iodine-123-IBZM Obtained by the Integral and Single-Scan Methods (n = 12)

AIMS scale	Integral method				Single-scan method				
	Spearman's		Pearson's		Spearman's		Pearson's		
	rho	p	r	p	rho	p	r	p	
Tremor	0.69	0.013	0.55	0.064	0.09	0.78	-0.01	0.98	
Bradykinesia	0.85	0.0004	0.77	0.004	-0.12	0.71	-0.07	0.83	
Rigidity	0.68	0.015	0.67	0.018	-0.13	0.69	-0.04	0.91	
Dystonia	0.72	0.008	0.57	0.052	0.13	0.68	0.22	0.49	
Total	0.82	0.0012	0.70	0.012	0.12	0.72	0.02	0.95	

rho = 0.69, p = 0.013; bradykinesia: rho = 0.85, p = 0.0004; rigidity: rho = 0.68, p = 0.015; dystonia: rho = 0.72, p = 0.008). Similarly, Pearson's linear correlation coefficients were significant for the total AIMS score (r = 0.7 p = 0.012) and the bradykinesia (r = 0.77, p = 0.004) and rigidity (r = 0.67, p = 0.018) subscales. In sharp contrast, differences in $f\text{-}B_{\text{unocc}}/K_d$ determined using the simulated single scan at 2 hr exhibit weak or even negative correlations with the total AIMS score and the four subscales; none of these correlations approach significance. Differences in $f\text{-}B_{\text{unocc}}/K_d$ did not correlate well or significantly with age, illness duration, or duration of drug exposure.

SPECT blood flow data acquired with ^{99m}Tc -HMPAO revealed no significant differences between the contralateral and ipsilateral sides in the subset of nine patients studied by this method. Table 5 summarizes the results of this analysis for the anatomical ROIs derived from coregistered MRI scans. Matched pair, two-tailed Student's t-tests did not find significant differences (minimum p > 0.13) between the contralateral and ipsilateral ^{99m}Tc -HMPAO data for either manner of normalization. The ^{99m}Tc -HMPAO blood flow data obtained by utilizing the same method of ROI analysis as was applied to the [^{123}I]IBZM scans are shown in Table 6. By this method of analysis and either approach to normalization, the ^{99m}Tc -HMPAO results for the contralateral and ipsilateral means are virtually identical. These ^{99m}Tc -HMPAO measures of blood flow also did not have any significant correlations

(minimum p > 0.37) with [^{123}I]IBZM results for the contralateral basal ganglia, the ipsilateral basal ganglia, or their difference when tested by either Spearman's rank test (best rho = 0.25) or Pearson's linear test (best r = -0.35).

DISCUSSION

The findings of this study support the hypothesis that [^{123}I]IBZM SPECT can provide clinically meaningful information about relative levels of extracellular dopamine as reflected by the availability of dopamine-D2 receptors. By applying the integral method of equilibrium analysis to [^{123}I]IBZM uptake in the basal ganglia of a diverse group of patients with Parkinson's disease and variable degrees of clinical asymmetry, we have been able to show a significant lateralization of receptor availability. This lateralization, which was not evident in a single time point SPECT analysis, correlated well and significantly with asymmetry of clinical signs, and it could not be explained by variations in regional cerebral blood flow as measured by ^{99m}Tc -HMPAO.

The present study differs in several other ways from previous imaging studies of radiolabeled D2 receptor antagonists in asymmetric Parkinson's disease. In the [^{123}I]IBZM SPECT study of Laulumaa et al. (24) and in the ^{11}C -raclopride PET study of Rinne (25), the patients were naive to dopaminergic drugs and had a shorter average duration of disease than the patients in the present study. Both studies found significantly increased ligand uptake in

TABLE 5
Means of Technetium-99m-HMPAO SPECT Blood Flow Data for Anatomical ROIs Derived from Coregistered MRI Scans (n = 9)*

Region	Normalized to dose (cpm/ml/mCi)		Normalized to brain slice (%)	
	Contralateral	Ipsilateral	Contralateral	Ipsilateral
Caudate	10.9 ± 1.1	11.4 ± 1.2	115 ± 8	118 ± 8
Putamen	12.9 ± 1.5	13.4 ± 1.3	132 ± 6	138 ± 5
Globus pallidus	11.3 ± 1.2	12.0 ± 1.3	115 ± 5	122 ± 6
Thalamus	11.5 ± 1.1	10.4 ± 1.0	120 ± 9	107 ± 5

*Values are mean ± s.e.m.

TABLE 6
Technetium-99m-HMPAO SPECT Blood Flow Data from the Same Method of ROI Analysis Applied to
Iodine-123-IBZM SPECT Scans

Subject no.	Normalized to dose (cpm/ml/mCi)		Normalized to occipital (%)	
	Contralateral	Ipsilateral	Contralateral	Ipsilateral
1	14.3	13.4	110	103
2	16.6	16.5	114	113
4	9.0	8.9	109	108
5	6.6	6.4	97	94
6	12.3	13	111	117
7	8.5	9.0	97	103
8	11.6	11.6	117	116
9	14.4	15.0	88	92
10	14.4	14.0	110	107
mean ± s.e.m	11.97 ± 1.12	11.99 ± 1.10	105.9 ± 3.2	106.1 ± 3.0
p value	0.92		0.90	

the basal ganglia of the contralateral side as compared to the ipsilateral side and attributed this increase to upregulation of dopamine-D2 receptors in the more affected basal ganglia. Yet, Rutgers et al. (26) detected no significant difference between the two sides of the brain in a study of both medicated and unmedicated patients with a longer average duration of illness. This latter study also found ¹¹C-methylspiperone uptake in the basal ganglia of medicated patients to be most similar to healthy controls, but significantly lower bilateral uptake in unmedicated patients. One possible explanation of these various findings would be an upregulation of dopamine-D2 receptors in the early stages of Parkinson's disease with a subsequent downregulation to more normal levels following treatment with dopaminergic medications. This hypothesis is supported by postmortem data suggesting dopamine-D2 receptor upregulation following nigral cell loss in parkinsonian patients that were not exposed to L-dopa before death (10,11,29,30), and by animal studies of nigrostriatal lesions indicating downregulation of this increase in dopamine-D2 receptors following L-dopa treatment (13). Thus, in the current study of medicated Parkinson's patients with a moderate average duration of illness, one might anticipate relatively normal concentrations of dopamine-D2 receptors in both contralateral and ipsilateral basal ganglia. The present study would, however, be sensitive to any lateralized differences in the concentration of extracellular dopamine which might arise during the period of medication abstinence preceding the SPECT study. This reasoning does, of course, assume that no significant upregulation of dopamine-D2 receptors occurs during the medication-free period. The short duration of abstinence (48 hr) from dopaminergic drugs makes receptor upregulation a less likely explanation for the observed asymmetry of [¹²³I]IBZM uptake than differences in local concentrations of striatal dopamine. The previous studies cited above would not have been sensitive to this effect, however, this interpretation must be regarded as speculative.

The observation by Rutgers et al. (26) of significantly

decreased bilateral uptake of ¹¹C-methylspiperone in unmedicated Parkinson's patients with a longer average duration of illness remains a paradox. The mean values of striatal-to-occipital ratios for [¹²³I]IBZM uptake in the present study are consistent with the values that have been obtained in previous studies in which patients with Parkinson's disease did not differ significantly from controls (14-17). A lack of difference between striatal [¹²³I]IBZM binding in parkinsonian patients and controls may indicate that survival of postsynaptic striatal neurons is an important diagnostic feature of idiopathic Parkinson's disease that can be estimated with available clinical imaging procedures. In this regard, however, it should be noted that the present study also suggests that single time-point measurements of [¹²³I]IBZM uptake might lack the sensitivity to detect these effects and a more robust method, such as the integral method presented here, may need to be employed.

It is also possible that some of these observations reflect early features of Parkinson's disease that become complicated by longer duration of illness, administration of dopaminergic drugs and aging. Some of the patients in the present study had also been exposed to antihypertensives and antiarrhythmic drugs that might possibly affect [¹²³I]IBZM uptake. Calcium channel antagonists, which were prescribed to several subjects in this study, have been shown to produce parkinsonism and reduced striatal [¹²³I]IBZM binding (36). It seems unlikely, however, that these medications would affect the hemispheres of the brain asymmetrically.

This study attempted in a preliminary and clinically accessible way to derive information about dynamic dopamine neurotransmission in patients with a disease process that affected the nigrostriatal dopaminergic pathways asymmetrically. The signal-to-noise ratio of the time-activity curves that were generated was often low. There are numerous and unpredictable sources of variability inherent in prolonged neuroimaging of human subjects. Data obtained in a 4-hr scanning protocol might conceivably be

influenced by many factors including the subject's emotional state, level of alertness and degree of motor activity. In addition, the relatively low specific-to-nonspecific ratio of [^{123}I]IBZM uptake and the relatively low count rates at later time points contribute to the variability of time-activity studies. In spite of these sources of variance, the integral method appears to be capable of generating useful measures of relative dopamine-D2 receptor availability from [^{123}I]IBZM SPECT data. This is most probably due a number factors including: (1) the reduction of random noise as the total counts accumulate in the integral; (2) elucidation of the optimum time points corresponding to the peak of specific binding for each subject; and (3) utilization of a maximal number peak time points in estimating the value of the peak specific binding. This method of linear estimation from a curve which is actually sigmoidal will certainly introduce a slight systematic underestimation of the actual peak value, but examination of the current data would suggest that the random deviations inherent in these data far exceeds these small errors. The method is also limited in the sense that estimates of specific kinetic parameters such as association and dissociation rates are not obtained, but in many studies, such as the present one, it is not clear that this additional information would contribute substantively to the a priori goals of the research. More complete kinetic modeling of [^{123}I]IBZM SPECT time-activity data parameters has been studied by others with the requisite chemical analysis of multiple blood samples to obtain an arterial input function and a single-slice SPECT camera that was capable of rapid acquisition of many time points (7). The results presented here suggest that, within the limits of its applicability, the integral method may be an efficacious alternative to more complete kinetic modeling.

Although the magnitude of the difference between dopamine-D2 receptor availability for the two sides of the brain was small, this observation is probably consistent with the natural progression of nigrostriatal cell loss in Parkinson's disease. Absolute clinical asymmetry is probably not associated with absolute asymmetry in surviving nigrostriatal cell numbers, since it is estimated that 50%–80% of nigrostriatal cells must be lost before clinical signs emerge (37).

Three subjects did not follow the predicted hypothesis. While two of the three subjects had lower degrees of clinical asymmetry (AI = 0.41), the other appeared to be quite asymmetric (AI = 1.00). The predictive failure in these three subjects also does not seem to be explained by age, illness duration or exposure to medications. Nevertheless, the significant correlations between lateralized $f\text{-}B_{\text{unocc}}/K_d$ differences and lateralized differences in measures of disease severity, suggest that the asymmetries observed by this method may have robust clinical meaning. These results compare quite favorably with correlations found between clinical severity, particularly for rigidity and bradykinesia, and striatal uptake of ^{18}F -fluoro-L-DOPA measured with PET scans (38–40). The particularly robust correlation of ^{18}F -fluoro-L-DOPA and [^{123}I]IBZM outcome

measures with measures of bradykinesia and rigidity is consistent with the clinical observation that these aspects of Parkinson's disease are the most responsive to L-dopa treatment.

CONCLUSION

Although SPECT imaging of dopamine uptake sites in patients with Parkinson's disease utilizing ^{123}I - β -CIT offers the advantages of lower nonspecific binding and the attainment of near-equilibrium conditions, and is thus perhaps more suitable for the differentiation of parkinsonian from normal striatal function, the relationship of ^{123}I - β -CIT uptake to endogenous dopamine concentrations and to clinical measurements has not yet been explored (41). The successful demonstration of strong clinical correlates of $f\text{-}B_{\text{unocc}}/K_d$ by means of the [^{123}I]IBZM SPECT technique used in this study may suggest that other diseases with putative dopaminergic abnormalities, such as Tourette's syndrome and schizophrenia, could also be examined.

REFERENCES

- Singhaniyom W, Tsai YF, Brucke T, et al. Blockade of in vivo binding of ^{125}I -labeled 3-iodobenzamide (IBZM) to dopamine receptors by D2 antagonist and agonist. *Brain Res* 1988;453:393–396.
- Kung HF, Pan S, Kung M, et al. In vitro and in vivo evaluation of [^{123}I]IBZM: a potential CNS D-2 dopamine receptor imaging agent. *J Nucl Med* 1989;30:88–92.
- Schonwetter BS, Luedtke RR, Kung M, et al. Characterization of membrane-bound and soluble D2 receptors in canine caudate using [^{123}I]IBZM. *J Pharmacol Exp Ther* 1989;250:110–116.
- Verhoeff NPLG, Bobeldijk M, Feenstra MGP, et al. In vitro and in vivo D2 dopamine receptor binding with [^{123}I]S(-)-iodobenzamide ([^{123}I]IBZM) in rat and human brain. *Nucl Med Biol* 1991;18:837–846.
- Costa DC, Verhoeff NPLG, Cullum ID, et al. In vivo characterization of 3-iodo-6-methoxybenzamide ^{123}I in humans. *Eur J Nucl Med* 1990;16:813–816.
- Kung HF, Alavi A, Chang W, et al. In vivo SPECT imaging of CNS D2 dopamine receptors: initial studies with iodine-123-IBZM in humans. *J Nucl Med* 1990;31:573–579.
- Seibyl JP, Woods SW, Zoghbi SS, et al. Dynamic SPECT imaging of dopamine D2 receptors in human subjects with iodine-123-IBZM. *J Nucl Med* 1992;33:1964–1971.
- Innis RB, Malison RT, Al-Tikriti M, et al. Amphetamine-stimulated dopamine release competes in vivo for [^{123}I]IBZM binding to the D2 receptor in nonhuman primates. *Synapse* 1992;10:177–184.
- Wong DF, Wilson AA, Chen C, et al. In vivo studies of [^{125}I]iodobenzamide and [^{11}C]iodobenzamide: a ligand suitable for positron emission tomography and single photon emission tomography imaging of cerebral D2 dopamine receptors. *Synapse* 1992;12:236–241.
- Lee T, Seeman P, Rajput A, et al. Receptor basis for dopaminergic supersensitivity in Parkinson's disease. *Nature* 1978;273:59–61.
- Rinne UK, Lonnberg P, Koskinen V. Dopamine receptors in the parkinsonian brain. *J Neural Trans* 1981;51:97–106.
- Pierot L, Desnos C, Blin J, et al. D1 and D2-type dopamine receptors in patients with Parkinson's disease and progressive supranuclear palsy. *J Neurol Sciences* 1988;86:291–306.
- Reches A, Wagner H, Jackson-Lewis V, et al. Chronic levodopa or pergolide administration induces down-regulation of dopamine receptors in denervated striatum. *Neurology* 1984;34:1208–1213.
- Cordes M, Hierholzer L, Schelosky L, et al. IBZM-SPECT imaging in Parkinson's disease. In: Narabayashi H, Nagatsu T, Yanagisawa N, Mizuno Y, eds. *Advances in neurology*, volume 60. New York: Raven Press, 1993:525–528.
- Oertel WH, Schwarz J, Tatsch K, et al. IBZM-SPECT as predictor for dopaminergic responsiveness of patients with de novo parkinsonian syndrome. In: Narabayashi H, Nagatsu T, Yanagisawa N, Mizuno Y, eds. *Advances in neurology*, volume 60. New York: Raven Press, 1993:519–524.
- Schwarz J, Tatsch K, Arnold G, et al. Iodine-123-iodobenzamide SPECT

- predicts dopaminergic responsiveness in patients with de novo parkinsonism. *Neurology* 1992;42:556-561.
17. Schwarz J, Tatsch K, Arnold G, et al. Iodine-123-iodobenzamide-SPECT in 83 patients with de novo parkinsonism. *Neurology* 1993;43(suppl):S17-S20.
 18. Schelosky L, Hierholzer J, Wissel J, et al. Correlation of clinical response in apomorphine test with D2 receptor status as demonstrated by ¹²³I-IBZM SPECT. *Mov Disord* 1993;8:453-458.
 19. Pizzolato G, Chierichetti F, Rossato A, et al. Dopamine receptor SPECT imaging in Parkinson's disease: a [¹²³I]IBZM and ^{99m}Tc-HMPAO study. *Eur Neurology* 1993;33:143-148.
 20. Oertel WH, Tatsch K, Schwarz J, et al. Decrease of D2 receptors indicated by ¹²³I-iodobenzamide single-photon emission computed tomography relates to neurological deficit in treated Wilson's disease. *Ann Neurol* 1992; 32:743-748.
 21. Schwarz J, Tatsch K, Vogl T, et al. Marked reduction of striatal dopamine D2 receptors as detected by ¹²³I-IBZM SPECT in a Wilson's disease patient with generalized dystonia. *Mov Disord* 1992;7:58-61.
 22. van Royen E, Verhoeff NFLG, Speelman JD, et al. Multiple system atrophy and progressive supranuclear palsy: diminished striatal D2 dopamine receptor activity demonstrated by ¹²³I-IBZM single photon emission computed tomography. *Arch Neurol* 1993;50:513-516.
 23. Ichise M, Toyama H, Fornazzari L, et al. Iodine-123-IBZM dopamine D2 receptor and technetium-99m-HMPAO brain perfusion SPECT in the evaluation of patients with and subjects at risk for Huntington's disease. *J Nucl Med* 1993;34:1272-1281.
 24. Laulumaa V, Kuikka JT, Soininen H, et al. Imaging of D2 dopamine receptors of patients with Parkinson's disease using single photon emission computed tomography and iodobenzamide I-123. *Arch Neurol* 1993;50:509-512.
 25. Rinne UK, Laihininen, Rinne JO, et al. Positron emission tomography demonstrates dopamine D2 receptor supersensitivity in the striatum of patients with early Parkinson's disease. *Mov Disord* 1990;5:55-59.
 26. Rutgers AWF, Lakke JPWF, Paans AMJ, et al. Tracing of dopamine receptors in hemiparkinsonism with positron emission tomography (PET). *J Neurolog Sci* 1987;80:237-248.
 27. Hoehn MM, Yahr MD. Parkinsonism: onset progression and mortality. *Neurology* 1967;17:427-442.
 28. Wyatt RJ. *Practical psychiatric practice, clinical interview forms, rating scales and patient handouts*. Washington: American Psychiatric Association Press; 1993.
 29. Seeman P, Bzowej NH, Guan HC, et al. Human brain D1 and D2 dopamine receptors in schizophrenia, Alzheimer's, Parkinson's and Huntington's diseases. *Neuropsychopharmacol* 1987;1:5-15.
 30. Guttman M. Receptors in the basal ganglia. *Can Neurol Sci* 1987;14:395-341.
 31. Kung MP, Kung H. Peracetic acid as a superior oxidant for preparation of [¹²³I]IBZM; a potential dopamine D-2 receptor imaging agent. *J Radio-pharm Lab Compd* 1989;27:691-700.
 32. Farde L, Eriksson L, Blomquist G, Halldin C. Kinetic analysis of central ¹¹C-raclopride binding to D2-dopamine receptors studied by PET-A comparison to the equilibrium analysis. *J Cereb Blood Flow Metab* 1989;9:696-708.
 33. Laruelle M, van Dyck C, Abi-Dargham A, et al. Compartmental modeling of iodine-123-iodobenzofuran binding to dopamine D2 receptors in healthy subject. *J Nucl Med* 1994;35:743-754.
 34. McGonigle P, Molinoff PB. Quantitative aspects of drug-receptor interactions. In: Siegel GJ, Agranoff BW, Albers RW, Molinoff PB, et al., eds. *Basic neurochemistry: molecular, cellular, and medical aspects*, 4th edition. New York: Raven Press; 1989:183-201.
 35. Bartko JJ, Carpenter WT. On the methods and theory of reliability. *J Nervous Mental Dis* 1976;163:307-317.
 36. Brucke T, Wober C, Harasko van der Meer C, et al. D2 receptor blockade by calcium antagonists measured with IBZM SPECT [Abstract]. *Soc Neurosci Abs* 1993;23:631.
 37. Jellinger K. The pathology of Parkinson's disease. In: Marsden CD, Fahn S, eds. *Movement disorders*, 2nd edition. London: Butterworths; 1987:124-165.
 38. Leenders K, Palmer A, et al. DOPA uptake and dopamine receptor binding visualized in the human brain in vivo. In: Fahn S, Marsden CD, Van Woert MH, eds. *Recent developments in Parkinson's disease*. New York: Raven Press; 1986:103-113.
 39. Guttman M, Stoessl J, Peppard RF, et al. Correlation between clinical findings and 6-(18F) fluorodopa PET in Parkinson's disease. *Neurology* 1987;37(suppl 1):329.
 40. Eidelberg D, Moeller JR, Dhawan V, et al. The metabolic anatomy of Parkinson's disease: complementary [¹⁸F]fluorodeoxyglucose and [¹⁸F]fluorodopa PET studies. *Mov Disord* 1990;5:203-213.
 41. Innis RB, Seibyl JP, Scanley BE, et al. Single-photon emission computed tomographic imaging demonstrates loss of striatal transporters in Parkinson disease. *Proc Natl Acad Sci* 1993;90:11965-11969.